HIGH-SPEED TWO-PHASE SRM FOR AN AIR-BLOWER DRIVE

Dong-Hee Lee, Kyungsung University; Hyunh Khac Minh Khoi, TOSY Robotics JSC; Jin-Woo Ahn, Kyungsung University

Abstract

In this study, the authors designed a high-speed, two-phase Switched Reluctance Motor (SRM) for an air blower. Considering high core loss at a maximum speed of 30,000 rpm for the proposed machine, a four-stator-pole two-rotor-pole (4/2) structure was chosen in order to reduce switching loss. Rotor pole shaping was employed because of a non-uniform air gap. Also, the rotor surface was optimally contoured in order to obtain constant torque and low torque ripple. The rotor pole arc had to be wide in such a way that torque ripple could be minimized during commutation. Iterative optimization using Finite Element Method (FEM) allowed the air gap to be designed for flat-top positive torque in phase excitation and small torque fluctuation during commutation. This SRM was designed with an asymmetric inductance profile where the positive region was wider than the negative one. The feasibility of the machine was verified by FEM and a prototype was built and installed in an air blower for experimental tests.

Introduction

Recently, there has been much interest in high-speed motor drives for practical applications to reduce system size while increasing efficiency. In particular, blowers, compressors, pumps, and spindle drives are suitable applications for the high-speed motor drives, and the demand for the high-speed motor system has greatly increased in the industrial market [1-4]. For practical systems, various electric machines, such as induction, permanent magnet, and switched reluctance motors, have been researched for application in high-speed systems [4-9].

SRM has a simple structure and inherent mechanical strength without rotor windings or permanent magnet. These mechanical structures are suitable for harsh environments and high-temperature and high-speed applications [4-12]. Raminosoa et al. [4] investigated a 6.5kW, 6/4 SRM with a speed rating of 14,000 rpm for a fuel-cell compressor. Also, an ultra-high-speed 6/4 SRM was introduced [5], where the practical results showed attainment of a speed of 150,000 rpm with a simple control scheme. That study used a 3-phase symmetric structure. An asymmetric staggered-gap type 4/2 SRM, with speeds up to 26,000 rpm, was also introduced [8-9]. In many speed drive systems, the number of poles is very important due to the electrical frequency and core losses. So, many high-speed drives use a two-pole system to reduce the electrical frequency. And, the number of phases is proportional to the drive cost [13-15]. Although the power losses are proportional to the switching frequency, the advance angle can introduce additional conduction and switching loss due to the excitation current building up without torque production; this advance area is proportional to the motor speed and phase numbers.

In this study, a 2-phase high-speed SRM was designed with continuous torque and self-starting characteristics. In order to reduce torque ripple, various types of rotor structure were analyzed. Additional non-linear air-gap structures were proposed based on the staggered-gap rotor type. The rotor pole shape provides a variable air gap according to rotor position, and it can produce a flat-top torque in a wide-torque region without torque dead-zone. In order to optimize torque ripple, the stator pole should have a cylindrical shape, but the shape of the rotor pole was designed by an iterative optimization process with FEM. The torque ripple, according to rotor position and air gap, was used as the optimal objective function. The final SRM had to have a non-uniform air gap and asymmetric inductance characteristic, which would yield wide positive and short negative torque regions. Such an SRM would be suitable for one-directional rotation due to its asymmetric inductance characteristic. The extended positive torque region can develop continuous torque with a torque overlap region and self-starting characteristics at any rotor position without torque dead-zone. And by optimizing the variable-air-gap structure, torque ripple can be reduced. In order to verify the performance of the proposed high-speed 4/2 SRM, computer simulations and experimental tests were employed.

Design of the Two-Phase 4/2 SRM

Conventional 4/2 SRM

The output torque, T_e , can be derived from the inductance, L , and phase current, i , as follows [1]:

$$T_e = \frac{1}{2} i^2 \frac{dL(\theta, i)}{d\theta} \tag{1}$$

where $L(\theta,i)$ is inductance and depends on both rotor position, θ , and phase current.

Figure 1 shows conventional and modified 4/2 SRMs. The modified types include a staggered-gap rotor pole surface type, air-teeth type, and air-hole rotor pole type [4], [13 -15]. Static torque profiles for those SRMs are compared in Figure 2, where the torque ripple is high, a zero-torque region is not avoidable, and torque for a motoring region is not enough in the conventional type.

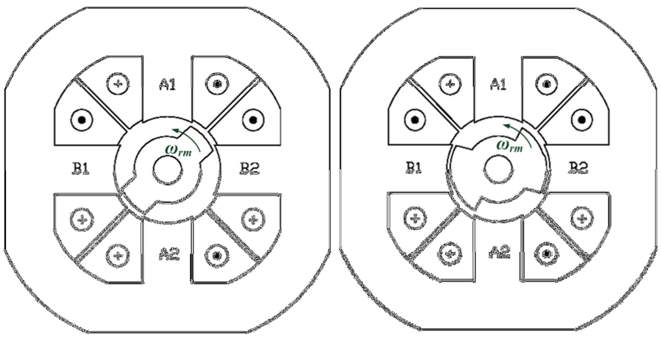

a) Conventional Type b) Staggered-Gap Type

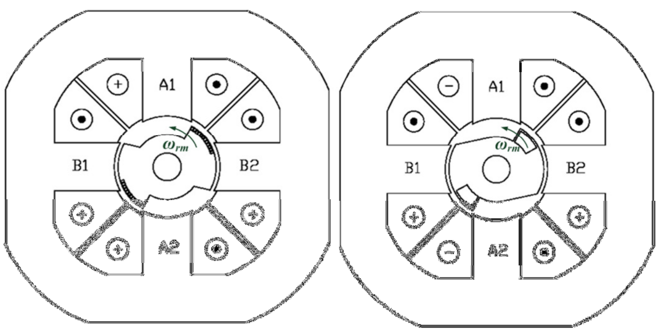

c) Air-Teeth Type d) Air-Hole Type

Figure 1. Various 4/2 SRMs

On the other hand, the modified designs are suitable for self-starting at any rotor position, due to a wide positive torque region. However, even with the modifications of the rotor poles, the SRMs still experience a sudden rise in positive torque region. The reason for this is an air-gap change on the rotor pole surface. The torque ripple causes high vibration and acoustic noise. An elaborate rotor pole shaping has to be incorporated with the design process instead of using one step on the rotor pole contour in order to obtain as small a torque fluctuation as possible. Among the modified types, the air-teeth and air-hole types are not easy to manufacture and to optimize. So, the design process is based on the staggered-gap rotor type. And, the rotor pole contour is determined to reduce torque ripple.

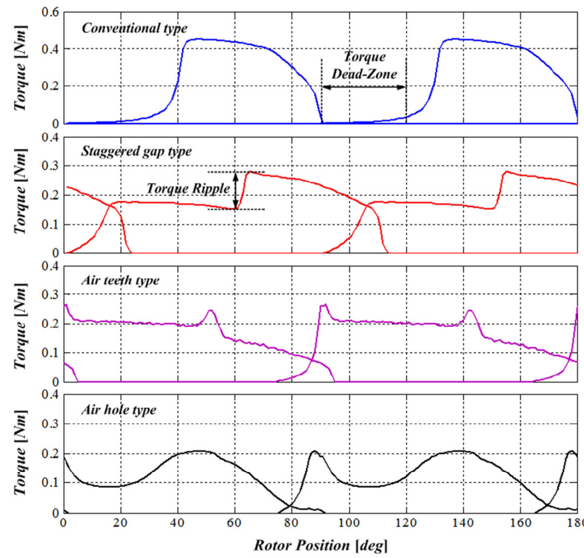

Figure 2. Static Torque Characteristics of Conventional, Staggered-Gap, Air-Teeth, and Air-Hole Types

Proposed 4/2 SRM

In order to obtain a wide positive torque region for stable self-starting, the rotor pole arc needs to be bigger than the stator pole pitch. Given this condition, the rotor pole surface must be optimally shaped, with respect to the rotor position, for mitigating torque ripple by means of an iterative method with FEM analysis.

Figure 3 illustrates the key design parameters in the determination of the rotor shape. The stator inner diameter (r_s) is determined to be constant. It can be seen that the rotor pole arc is wider than one stator pole pitch. One rotor pole is segmented into *n* nodes, with each segment having its own radius (r_k) and angular position (φ_k) in polar coordinates. Angle increment (Dφ) is determined by two node numbers and the rotor pole arc. The length of the air gap at the *k*-th node is equal to the difference between r_s and r_k. Radius r_k changes within a limited boundary to achieve less torque oscillation. At the *k*-th node, radius r_k needs to be decreased in case the calculated torque is bigger than the desired one. Conversely, if the calculated torque is too small, the radius r_k is increased until the calculated torque reaches the target. It should be noted that the maximum possible value for radius r_k is limited by a critical dimension, which is the minimum air gap.

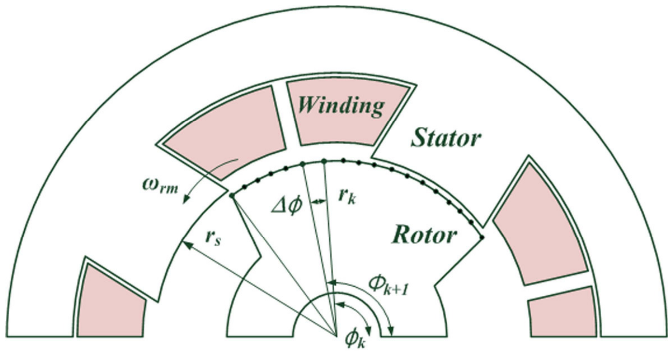

a) Initial Condition

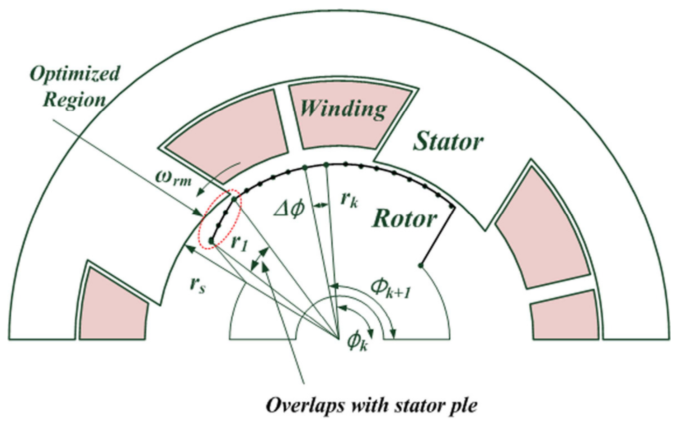

b) Optimization Process

Figure 3. Key Parameters in Rotor Shape Optimization

Figure 4 shows the step-by-step design algorithm of rotor pole shaping. The initial set of conditions is: minimum air gap, acceptable torque error T_{err} [%] as a percentage of average torque T_{avg}, a node number, and angle increment Dφ. In this study, the angle increment was one degree and the acceptable torque error was set to 2%. Rated torque was set at 0.2Nm for a 600W, 30,000 rpm high-speed air-blower system.

Figure 5 shows the flux distribution and density during optimization. The output torque was affected by both air-gap and fringing flux. In general, the amount of fringing flux—when the rotor was optimized at the *k*-th node—will change when the (*k*+1)-th node is being optimized. This means that optimization of subsequent nodes will change torques at previous nodes which were calculated in previous steps. However, air-gap flux dominates fringing flux. The fringing effect can be ignored. So, the nodes were considered to be independent of each other during the optimization process.

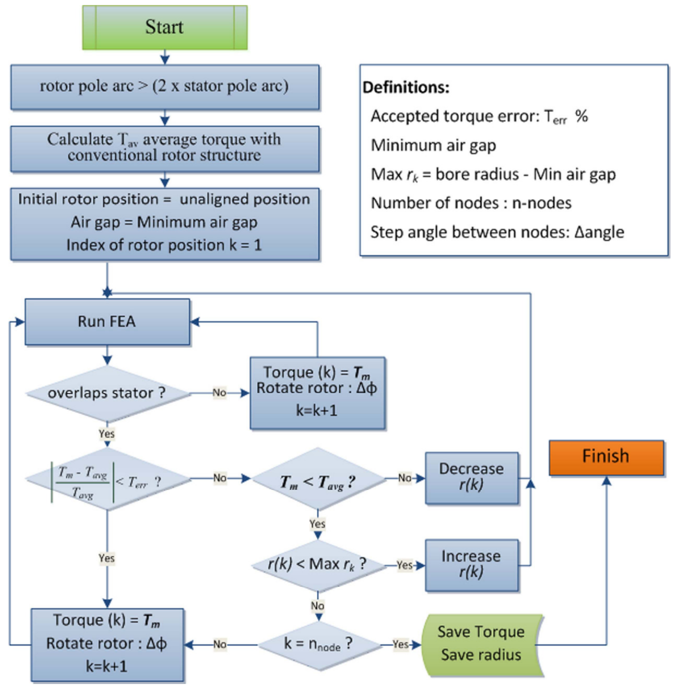

Figure 4. Flow Chart for Rotor Pole Optimization

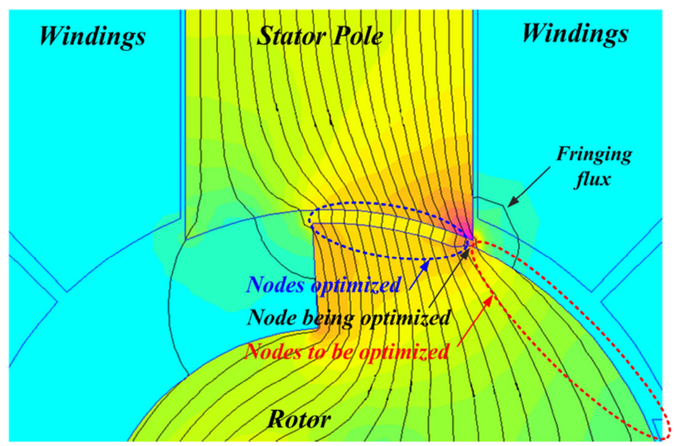

Figure 5. Flux Distribution During Optimization

Figure 6 shows the results of rotor pole shaping through the optimization procedure for the high-speed 4/2 SRM, and Table 1 shows the specifications of the motor.

Table 1. Specifications of the Proposed 4/2 SRM

Parameters	Value	Parameters	Value
Output power	600W	Average Torque	0.2Nm
Stator Poles	4	Rotor Poles	2
Bore Diameter	30mm	Stator Outer Dia	80mm
Stack Length	30mm	Air-gap	0.25mm
Stator Pole Arc	46°	Rotor Pole Arc	102°

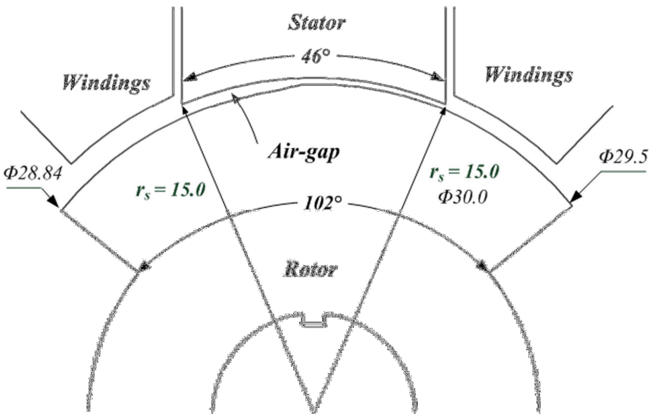

Figure 6. Optimized Rotor Pole Shape

Figure 7 shows the inductance and torque profiles of the prototype SRM analyzed by FEM. Table 1 shows the design sheet and specifications of the motor. The inductance is asymmetric and, hence, the machine can produce a wide positive torque region for continuous torque generation. In order to include the saturation effect of the steel, the design procedure was conducted at a current of 7A. As shown in Figure 7, the inductance profiles are almost linear in the low -current region, and the corresponding torque can be considered to be constant. However, in the high-current region, the torque is decreased at the middle of the rotor poles due to the steel saturation.

As seen in Figure 7b, FEM results show higher torque ripple than the target value in the middle position of the rotor. In the design process, the maximum torque ripple was set to 2% of the rated value. However, the analyzed maximum torque ripple was about 10%.

In Figure 8, static torque profiles of three 4/2 SRMs are compared. The structure of the conventional 4/2 SRM is shown in Figure 1a, with the modified type shown in Figure 1b. The motors being compared were redesigned with the same size and output power for the proposed application. The proposed SRM has lower torque ripple than conventional and modified 4/2 SRMs. In the proposed design, torque during commutation secures stable self-starting at any rotor position without torque dead-zone. The analyzed torque ripple was under 10% at the rated conditions. Due to the limit of the minimum air gap around the mid-point of the rotor pole, the analyzed torque ripple was higher than the desired one. As shown in Figure 6, the variable air gap converges to the minimum air gap to improve the output torque. So, the torque ripple around the mid-point of the rotor pole arc would be higher than the expected value. However, the proposed prototype SRM had much lower torque ripple than the modified SRM, which had more than 60% torque ripple at the rated conditions.

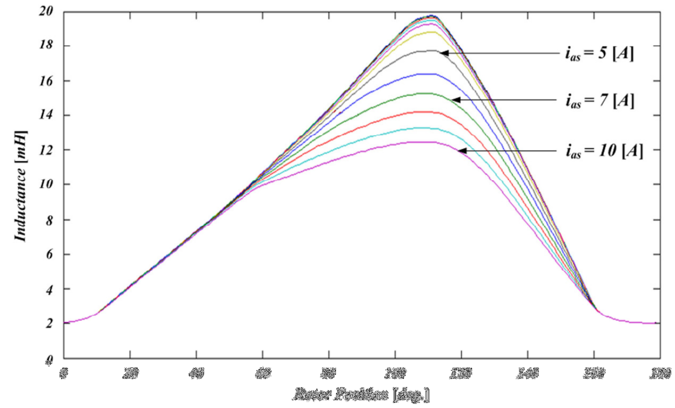

a) Inductance Profile of the Proposed SRM

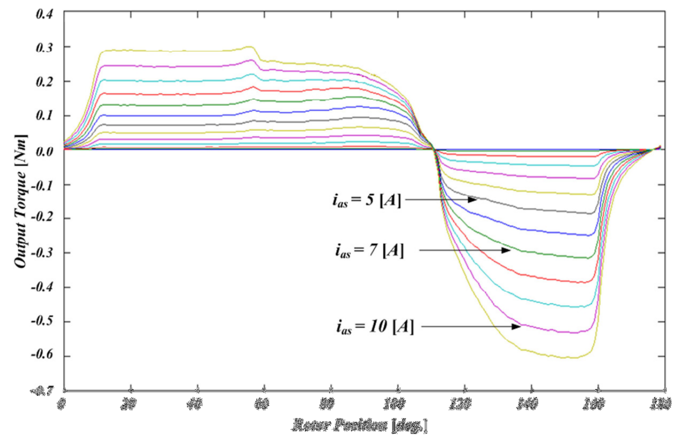

b) Torque Profile of the Proposed SRM

Figure 7. Inductance and Torque Characteristics of the Proposed 4/2 SRM

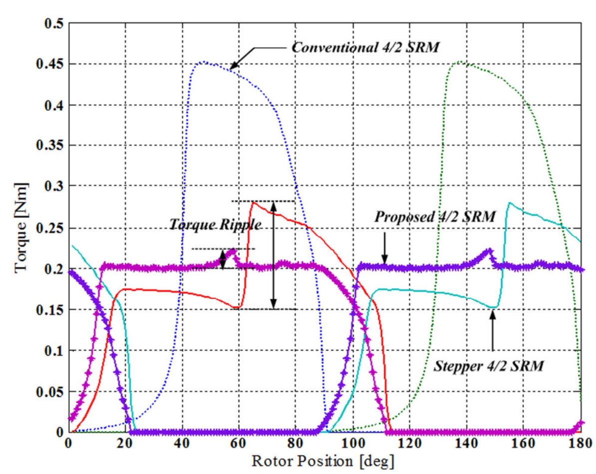

Figure 8. Torque Characteristics Comparison

Simulation and Experimental Results

In order to verify the performance of the proposed motor, dynamic simulation using Matlab was performed on the practical air-blower system. Figure 9 shows simulation results at the rated speed. In the simulation results, the proposed motor can operate well in the range of 15,000 to 30,000 rpm. Torque ripple during single-phase excitation was significantly small, but the ripple becomes high during commutation due to constant current control.

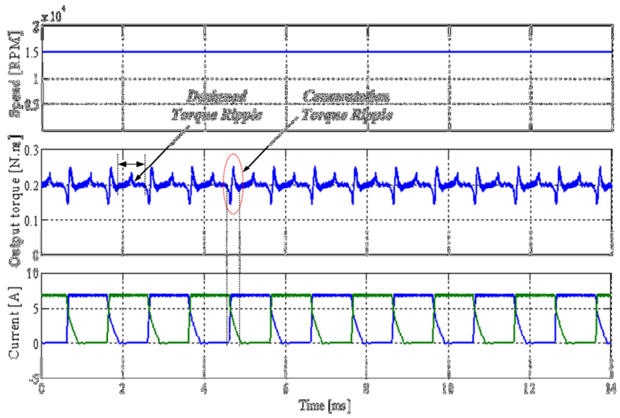

a) 15,000 rpm

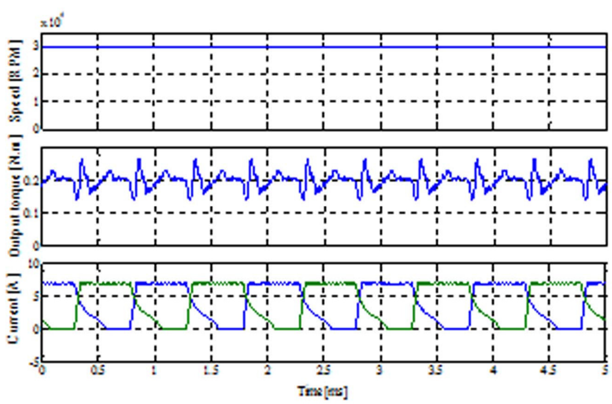

b) 30,000 rpm

Figure 9. Simulation Results at Rated Torque

Figure 10 shows a prototype motor including the rotor, stator, and motor assembly. Figure 11 shows the experimental configuration, including the motor assembly. A two-phase asymmetric converter and DSP (TMS320F-2811) were used for motor control. The asymmetric converter was designed with MOSFETs and power diodes that have 600V, 50A ratings. Current was detected by a mounted-chip type current sensor (ACS712) and embedded 12-bit ADC of the DSP.

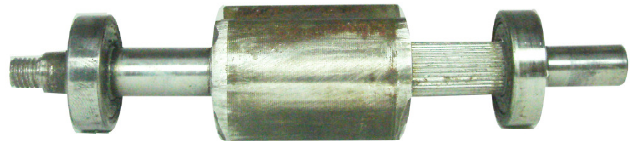

a) Rotor

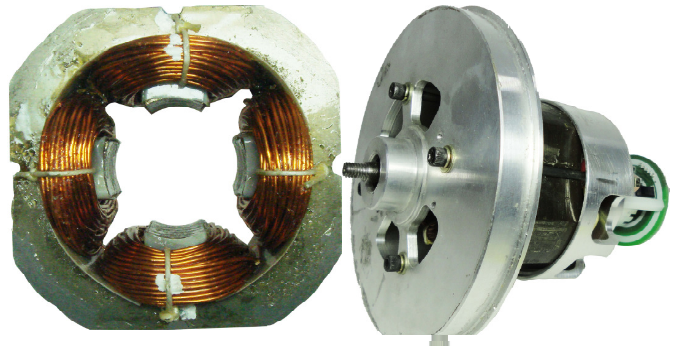

b) Stator **c) Assembled SRM**

Figure 10. Prototype of 4/2 SRM

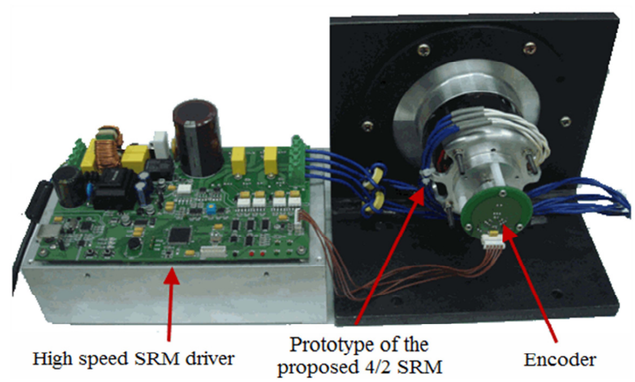

Figure 11. Experimental Configuration

Balanced, soft-chopping technology was used for the switching of the asymmetric converter to reduce the current ripple in the phase winding. There were 16 pulses per revolution from an ultra-fast photo-interrupter, and the signal was connected to the QEP module of the DSP. The motor controller can count 64 pulses per revolution with a phase detecting signal.

Figure 12 shows the measured torque characteristics of the proposed high-speed 4/2 SRM. The desired torque was the theoretically analyzed value. The SRM had higher torque ripple than expected. The reason for this was manufacturing error in the rotor and stator. From the practical measurements, the rotor diameter had 1% error. Furthermore, the assembly of the stator and bracket had distortion in the rotational direction. This distortion introduced a concentricity error between the stator and rotor assembly. For these reasons, the measured torque had some errors.

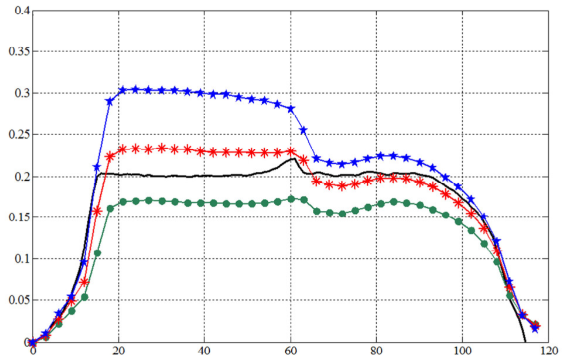

Figure 12. Measured Torque Characteristics

Figures 13 through 15 show the experimental results using the dynamometer. Figure 13 shows a no-load operation at 10,000 and 30,000 rpm. The proposed motor does a good job of tracking the reference speed. Radial vibration increased greatly in the high-speed region.

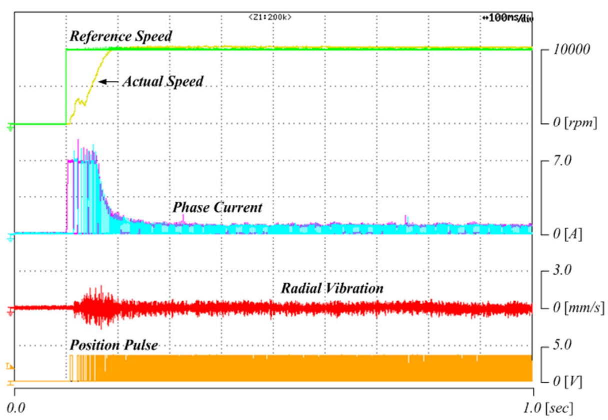

a) 10,000 rpm

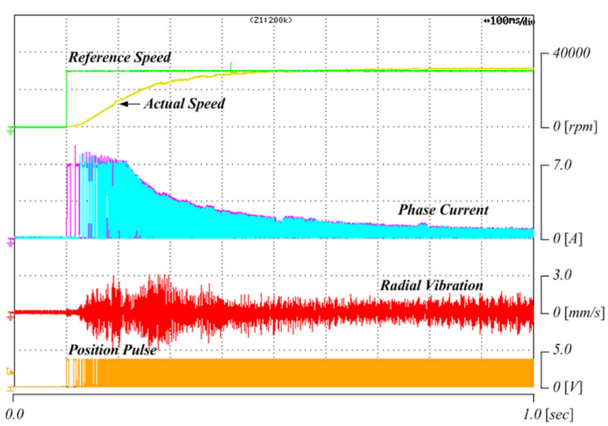

b) 30,000 rpm

Figure 13. Experimental Results under No-Load Operation

Figure 14 shows the experimental results according to the load variation at 10,000 and 30,000 rpm. As shown in the experimental results, the designed motor can operate quite well over a wide speed range.

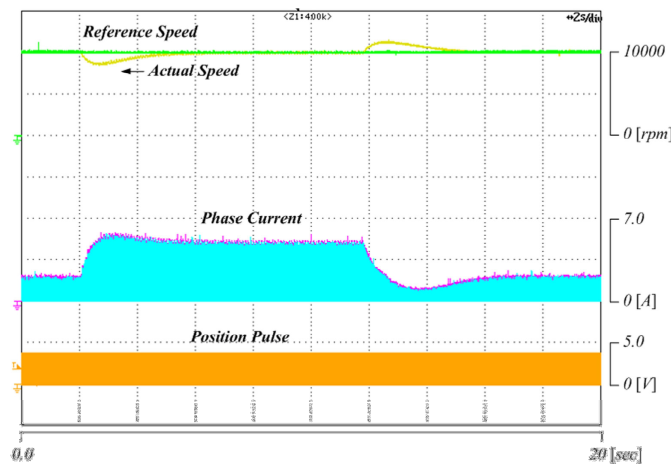

a) 10,000 rpm

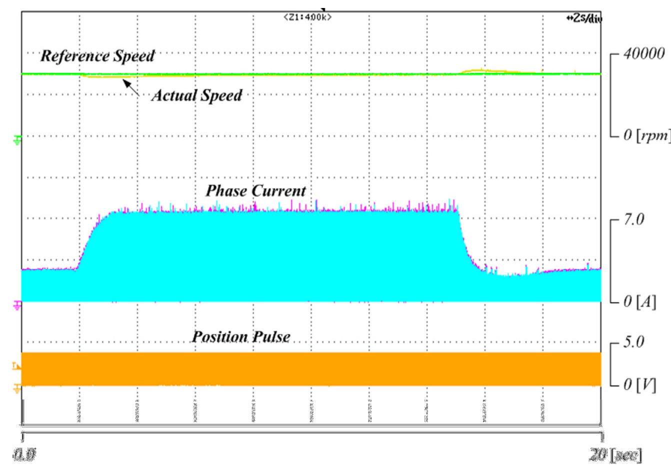

b) 30,000 rpm

Figure 14. Experimental Results with Load Variation

Figure 15 shows the experimental results of the designed motor used to drive a practical air blower. Impeller type 1 was used in the conventional design. The output air pressure was almost the same as that of a conventional air blower in which a universal motor would be installed, and the mechanical vibration and acoustic noise were lower than that of the conventional air blower.

Figure 16 shows the operating characteristics of an air-blower with the proposed SRM and impellers. As shown here, the Impeller Type 1 is for low-speed motors with high air pressure, while Impeller Type 2 is for high-speed motors with low air pressure.

Conclusion

This paper presents a study of a high-speed 4/2 SRM, where rotor pole shape was optimized for torque ripple reduction. The outer dimensions were the same as those of a conventional air-blower motor. In order to guarantee continuous torque at any rotor position, the positive torque region had to be extended by an asymmetric inductance profile of the motor. That is possible because the blower rotates in one direction. The rotor pole shaping was carried out by an iterative optimization procedure using FEM. The proposed motor was verified in terms of the capability of wide speed operation by air-blower tests in which it demonstrated high-efficiency and low-vibration characteristics.

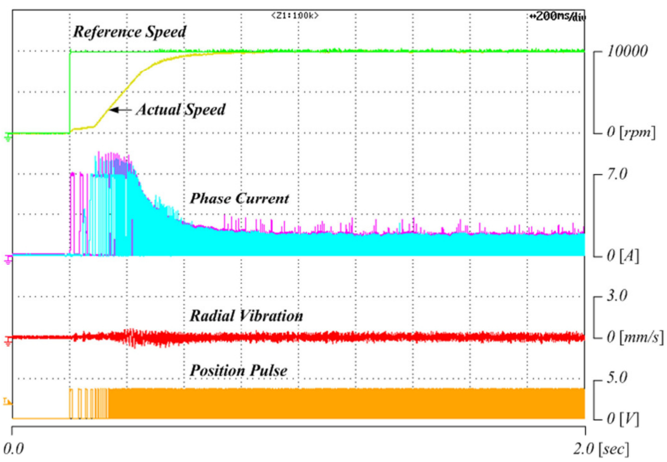

a) 10,000 rpm

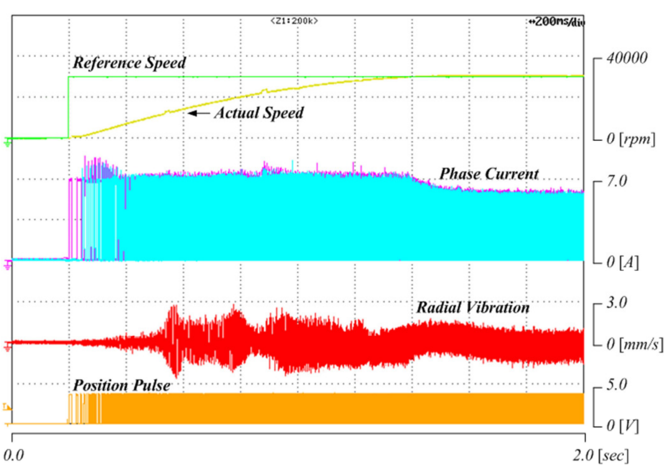

b) 30,000 rpm

Figure 15. Experimental Results with a Practical Air-Blower

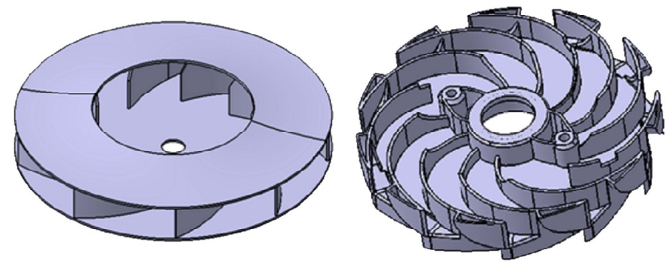

a) Impeller Type 1

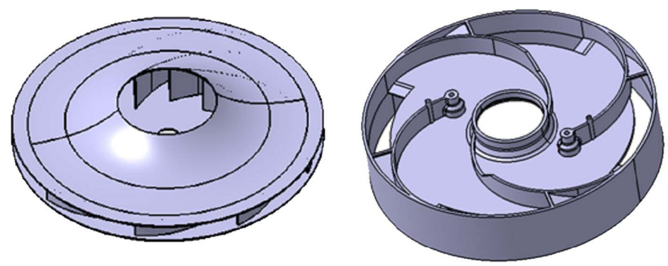

b) Impeller Type 2

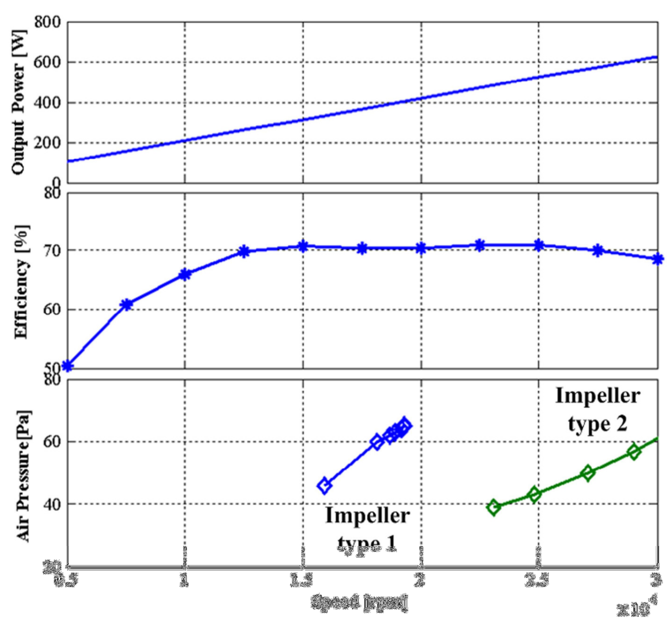

c) Measured Power, Efficiency, and Air Pressure

Figure 16. Operating Characteristics of Air-Blower with Proposed SRM

Acknowledgements

This work was supported by Energy Resource R&D program (2009T100100654) under the Ministry of Knowledge Economy, Republic of Korea.

References

[1] Krishnan, R. (2001). *Switched Reluctance Motor Drives: Modeling, Simulation, Analysis, Design, and Application*. CRC Press.

[2] Bianchi, N., Bolognani, S., & Luise, F. (2006) High speed drive using a slotless PM motor. *IEEE Transaction on Power Electronics*, 21(4), 1083-1090.

[3] Hanoun, H., Hilairet, M., & Marchand, C. (2010). Design of an SRM Speed Control Strategy for a Wide Range of Operating Speeds. *IEEE Transaction on Industrial Electronics*, 57(9), 2911-2921.

[4] Raminosoa, T., Blunier, B., Fodorean, D., & Miraoui, A. (2010). Design and Optimization of a Switched Reluctance Motor Driving a Compressor for a PEM Fuel-Cell System for Automotive Applications. *IEEE Transaction on Industrial Electronics,* 57(9), 2988-2997.

[5] Kozuka, S., Tanabe, N., Asama, J., & Chiba, A. (2008). *Basic characteristics of 150,000r/min switched reluctance motor drive*. Power and Energy Society General Meeting - Conversion and Delivery of Electrical Energy in the 21st Century, (pp. 1-4).

[6] Mademlis, C., & Kioskeridis, I. (2010). Gain-Scheduling Regulator for High-Performance Position Control of Switched Reluctance Motor Drives. *IEEE Transaction on Industrial Electronics*, 57(9), 2932-2938.

[7] Kajiwara, K., Kim, Y. J., & Dohmeki, H. (2007). Analysis of the maximizing start torque of Switched Reluctance Motor for super high speed drive. *Proceedings of the ICEMS 2007,* (pp. 1428-1432).

[8] Genda, T., & Dohmeki, H. (2009). Characteristics of 4/2 Switched Reluctance Motor for a high speed drive by the excitation angle. *Proceedings of the ICEMS 2009*, (pp. 1-6).

[9] Kartono, I. R., Kajiwara, K., & Dohmeki, H. (2008). Dynamic simulation of maximizing the starting torque for super-high-speed drive of a 4/2 Switched Reluctance Motor. *Proceedings of ICEM 2008,* (pp. 1 -6).

[10] Ahn, J. W., Kim, T. H., & Lee, D. H. (2005). Performance of SRM for LSEV. *Journal of Power Electronics*, 5(1), 45-54.

[11] Lee, D. H., Lee, Z. G., Liang, J., & Ahn, J. W. (2007). Single-Phase SRM Drive With Torque Ripple Reduction and Power Factor Correction. *IEEE Transaction on Industry Applications*, 43(6), 1578-1587.

[12] Ohyama, K., Naguib, M., Nashed, F., Fujii, K., & Uehara, H. (2006). Design using finite element analysis of a switched reluctance motor for electric vehicle. *Journal of Power Electronics*, 6(2), 163-171.

[13] Faiz, J., Finch, J. W., & Metwally, H. M. B. (1995). A novel switched reluctance motor with multiple teeth per stator pole and comparison of such motors. *Electric Power Systems Research*, 34, 197-203.

[14] Kano, Y., Kosaka, T., & Matsui, N. (2010). Optimum Design Approach for a Two-Phase Switched Reluctance Compressor Drive. *IEEE Transaction on Industry Applications*, 46(3), 955-964.

[15] Oh, S. G., & Krishnan, R. (2006). Two Phase SRM with Flux Reversal Free Stator: Concept, Analysis, Design and Experimental Verification. *Conference Record of The 2006 IEEE Industry Applications Conference 41st IAS Annual Meeting,* (pp. 1155-1162).

Biographies

DONG-HEE LEE received his B.S., M.S. and Ph.D. in Electrical Engineering from Pusan National University, Pusan, Korea, in 1996, 1998 and 2001, respectively. He worked as a Senior Researcher in the Servo R&D Team at OTIS-LG, from 2002 to 2005. He has been with Kyungsung University, Busan, Korea, as an Associate Professor in the Department of Mechatronics Engineering since 2005. He is visiting professor of University of Wisconsin (WEMPEC) in 2012. His current research interests include Power Electronics and motor control systems. His email address is leedh@ks.ac.kr

HUYNH KHAC MINH KHOI received his B.S. in Electrical Engineering from the University of Technology, Ho Chi Minh City, Vietnam, in 2007 and his M.S. in Electrical Engineering from Kyungsung University, Busan, Korea, in 2010. Since 2010, he has been with the Electronics Department, TOSY Robotics JSC., Hanoi, Vietnam where he is currently a R&D Engineer. His current research interests include the design and advanced control of electrical machines, and power electronics.

JIN-WOO AHN received his B.S., M.S. and Ph.D. in Electrical Engineering from Pusan National University, Busan, Korea, in 1984, 1986, and 1992, respectively. He has been with Kyungsung University, Busan, Korea, as a Professor in the Department of Mechatronics Engineering since 1992. He was a Visiting Researcher in the Speed Lab at Glasgow University, U.K., a Visiting Professor in the Dept. of ECE and WEMPEC at the University of Wisconsin-Madison, USA, and a Visiting Professor in the Dept. of ECE at Virginia Tech, from 2006 to 2007. He is the author of five books including SRM, the author of more than 120 papers and has several patents. His current research interests include advanced motor drive systems and electric vehicle drives.